

Enhancement of Small Telescope Images Using Super-Resolution Techniques

R. Marsh

Computer Science Department, University of North Dakota, Grand Forks, ND 58202

`rmarsh@cs.und.edu`

T.R. Young

Physics Department, University of North Dakota, Grand Forks, ND 58202

`tim_young@und.edu`

and

T. Johnson and D. Smith

Physics Department, University of North Dakota, Grand Forks, ND 58202

ABSTRACT

We present the results of our study into the feasibility of using super-resolution techniques to enhance the quality of images obtainable with small telescopes. With super-resolution one acquires a series of images of a moving object such that the object of interest is only slightly displaced in each image. One then uses statistical methods to combine these separate images to produce a sub-pixel interpolation of the original image. The methodology has been successfully demonstrated in several application areas and can theoretically double (or more) the image spatial resolution. Our interest is whether or not the wander resulting from atmospheric turbulence creates sufficient displacement for the super-resolution algorithm.

Subject headings: techniques: image processing

1. Introduction

One factor affecting the quality of images obtained by ground based telescopes is atmospheric turbulence. Random index-of-refraction fluctuations, caused by atmospheric turbulence results in the optical path length of the atmosphere to change in both space and time

producing random aberrations at the telescope focal plane that degrade (blur) and displace (wander) the image. For exposure times shorter than the evolution time of the phase inhomogeneities, each patch of the wavefront with diameter r_0 would act independently of the rest of the wavefront resulting in many bright spots, or speckles, spread over the area defined by the long exposure image. These speckles can occur randomly along any direction within an angular patch of diameter $1.22/r_0$. Whether blur or wander dominates the degradation is driven by the ratio D/r_0 , where D is the telescope diameter and r_0 is Fried's parameter or coherence length. For $D/r_0 \leq 3$ the bulk of the energy (from a star) is contained in a near diffraction limited wandering speckle. For larger D/r_0 turbulent blurring progressively dominates over wander (Tatarskii & Zavorotny 1993).

One technology used to reduce the degradation caused by atmospheric turbulence is adaptive optics where the correction of the aberration is done before an image is acquired. The three main elements in adaptive optics are the wave-front sensor, the deformable mirror, and a controller. While popular, adaptive optics have drawbacks as the current commercial adaptive optics systems require the telescope to continually and rapidly track (via some mechanical means) the object of interest while acquiring the image. Additional factors that degrade the adaptive optical imaging system performance are finite light levels in the wave fronts associated with anisoplanatism. Anisoplanatism occurs when the wave-front sensor and the object of interest must pass through different columns of air which in turn limits the correctable field of view of the adaptive optics. Several other factors are finite spatial sampling of the wave-front sensor, finite number of degrees of freedom available with the deformable mirror, and the finite temporal response of the adaptive optical imaging systems (Troxel et al. 1995). Finally, this technology is somewhat expensive and infeasible for the multitudes of smaller telescopes that exist.

Additional technologies used to reduce the degradation caused by atmospheric turbulence include a variety of image processing methods such as interlacing, shift-and-add, and the Drizzle method (Fruchter & Hook 2002).

In addition to atmospheric turbulence, digitally acquired telescope images suffer a loss of high frequency detail due to detector imposed undersampling and the telescope's point-spread function (PSF). Therefore, when a portion of the sky S is observed by a ground-based telescope, it is convolved by the point-spread function (PSF) of the optics O , by the response function of the detector pixels P , and by a myopic point-spread function T due to atmospheric turbulence producing an image, $I = S \otimes O \otimes P \otimes T$, where \otimes is the convolution operator. Fortu-

nately, many deconvolution approaches have been developed to reduce these affects (Starck & Pantin 2002).

This paper focuses on the enhancement of astronomical images acquired by a telescope using super-resolution techniques. The general idea behind super-resolution is to acquire images of a moving object such that the object of interest is only slightly displaced in each image and to use statistical methods to combine these separate images to produce a sub-pixel interpolation of the original image(s). While the technology has been successfully demonstrated in several application areas and can theoretically double (or more) the image resolution, the issue here is whether or not the wander resulting from atmospheric turbulence creates sufficient displacement.

2. Background

Super-resolution was originally introduced by Tsai and Huang (1984) in which an observation model was defined for an image sequence consisting of subpixel shifts of the same scene. They relied on a pseudo-inverse least-squares technique to regularize the problem when all required subpixel shifts of the scene were not available, and thus, a direct inversion could not be determined. Patti, Sezan and Tekalp (1995) developed a projection onto convex sets algorithm that computes an estimate from noisy observations obtained by shifting or rotating a scene with respect to the detector plane. Finally, Schultz and Stevenson (1996) and Cheeseman, Kanefsky, Kraft, Stutz, and Hanson (1996) separately introduced Bayesian methods to integrate the image sequence.

Enhancement algorithms refer to an up-sampling factor ($\uparrow n$), the degree by which an image is to be enlarged in both directions. Several popular methods exist for the interpolation of images, including zero-order hold up-sampling, bilinear interpolation, cubic B-spline interpolation, and Bayesian maximum a posteriori (MAP) estimation (Schultz & Stevenson 1994). Unfortunately, these methods generate similar results. To extract additional detail from an image, a sequence of images (video frames) must be acquired at temporal intervals such that object or scene movement occurs. In essence, super-resolution enhancement exploits the temporal correlations present between under-sampled video frames to improve spatial resolution. Substantial detail can be extracted, provided that there is a great deal of subpixel overlap from frame-to-frame. The Bayesian high-resolution video stills (HRVS) algorithm (Schultz & Stevenson 1996) uses motion vectors estimated by subpixel-resolution block matching to compute enhanced video frames with greater detail than those estimates

generated by single image interpolation methods.

The goal of the general super-resolution enhancement problem is to estimate an unknown high-resolution image given a short low-resolution video sequence. Assume that the k^{th} image within an image sequence, denoted as

$$F = \left\{ \mathbf{f}^{(m)}, \dots, \mathbf{f}^{(k)}, \dots, \mathbf{f}^{(n)} \right\} \text{ for } m \leq k \text{ and } k \leq n, \quad (1)$$

has been selected for enhancement. Super-resolution enhancement is achieved through the temporal integration of pictures containing subpixel transformations, such that an estimate of the unknown frame, $\mathbf{u}^{(k)}$, is computed from neighboring images within the subsequence. The video observation model that takes into account pixel displacements between $\mathbf{f}^{(l)} \in F$, for $l \neq k$ and the frame to be enhanced, $\mathbf{f}^{(k)}$, is given as

$$\mathbf{f}^{(l)} = \underline{\mathbf{A}}^{(l,k)} \mathbf{u}^{(k)} + \mathbf{n}^{(l,k)} \quad (2)$$

in which the linear operator, $\underline{\mathbf{A}}^{(l,k)}$, both subsamples the high-resolution frame and incorporates the subpixel displacements between frames, and $\mathbf{n}^{(l,k)}$ is an independent and identically distributed Gaussian random vector representing the error in estimating $\underline{\mathbf{A}}^{(l,k)}$ from $\mathbf{f}^{(k)}$ and $\mathbf{f}^{(l)}$. The notation $\mathbf{f}^{(l)}$ denotes those pixels within $\mathbf{f}^{(l)}$ that are observed entirely from the motion-compensated elements of $\mathbf{u}^{(k)}$. Using a Huber-Markov random field model for piece-wise smooth image data, the high-resolution frame can be computed as the following Bayesian maximum a posteriori (MAP) estimate:

$$\mathbf{u}^{(k)} = \min_{\mathbf{u}^{(k)} \in U} \left\{ \sum_{p \in P} \sum_{i=1}^4 \rho_{T_h}(\mathbf{d}'_{p,i} \mathbf{u}^{(k)}) + \sum_{\substack{\mathbf{f}^{(l)} \in F \\ l \neq k}} \lambda^{(l,k)} \|\mathbf{f}^{(l)} - \underline{\mathbf{A}}^{(l,k)} \mathbf{u}^{(k)}\|^2 \right\} \quad (3)$$

In the above expression, the constraint set is defined as

$$U = \left\{ \mathbf{u}^{(k)} : \mathbf{f}^{(k)} = \mathbf{A}^{(k,k)} \mathbf{u}^{(k)} \right\} \quad (4)$$

Since displacement vectors are not required for only subsampling $\mathbf{u}^{(k)}$, $\mathbf{A}^{(k,k)}$ is not an estimate. The (smoothing) parameter $\lambda^{(l,k)}$ represents the confidence in estimating $\underline{\mathbf{A}}^{(l,k)}$, constructed using the subpixel-resolution displacements estimated from $\mathbf{f}^{(l)}$ with respect to

$\mathbf{f}^{(k)}$. Finite differences, $\mathbf{d}_{p,i} \mathbf{u}^{(k)}$, are used to represent second-order spatial derivatives at each pixel location $\mathbf{p} = (p1, p2, \dots)$, with horizontal, vertical, and diagonal orientations. The Huber edge penalty function is used to preserve discontinuities, given by the expression

$$\rho_{T_H}(\tau) = \begin{cases} \tau^2, & |\tau| \leq T_H, \\ 2T_H |\tau| - T_H^2, & |\tau| > T_H. \end{cases} \quad (5)$$

The Huber function threshold parameter, T_H , controls the size of the discontinuities within the data. Since the objective function in (4) is convex, the gradient projection algorithm is used to efficiently compute the unique estimate $\mathbf{u}^{(k)}$ (Schultz & Stevenson 1996).

3. The Method

Experience has shown that the best results are obtained when five images have been acquired such that they overlap in a manner forming a "Z" pattern, as shown in Figure 1, and such that the amount of overlap is 0.5 pixels in both the vertical and horizontal axis. Experience has also shown that T_H should be in the range ($1.0 \leq 10.0$). However, the selection of T_H is highly dependent on the quantity and magnitude of the edges in the images. Finally, experience has also shown that λ should be in the range ($1.0 \leq 100.0$). As λ is decreased the image is smoothed more in an effort to reduce the affects of noise on the estimation of the enhanced image.

Since the question we were interested in answering was whether or not the random wander resulting from atmospheric turbulence creates sufficient displacement and displacement in the proper directions, our first task was to generate an algorithm that would determine the center of mass of each image. The center of mass data was then used to identify the "reference" image (the most central image of the set) and to determine the amount of displacement of each image from the reference image ($\mathbf{A}^{(l,k)}$). Ideally, the displacement would be 0.5 pixels. However, any displacement amount of $N.5$, where N is some integer, would also suffice as a simple translation algorithm could remove the integer component of the displacement. Once the reference image is selected and the displacements adjusted the super-resolution algorithm of Schultz and Stevenson (1996) is applied.

4. Examples

In this section we present results using the method developed for three different astronomical objects. For each object five images were acquired using a SBIG ST-2000XM CCD Camera and a Meade 12" LX200GPS telescope that has a focal length of 3048mm and a f-ratio of f/10. The images were acquired in rapid succession using the maximum resolution of the camera (1600x1200 pixels). These images are referred to as the reference images R and were used to derive a quantitative image improvement value. A set of lower resolution images (800x600 pixels) was generated from the reference images by integrating over 2x2 non-overlapping pixel neighborhoods. These downsampled images are referred to as the original images O, are the images that were processed by the super-resolution software, and represent the undersampled/lower resolution images that would typically be acquired by a telescope. The resulting images are referred to as the super-resolution images S. Exposure times varied for each object, but were in the range of one to ten seconds. Finally, for these results $T_H = 3D$ 1.0 and $\lambda = 10.0$.

In Figures 2a, 2b, 2c, 3a, 3b, 3c, and 4a, 4b, 4c below, the images are subsections of the centermost image of each five image set magnified by a factor of two (to show the improvements in greater detail). The quantitative image improvement I is calculated using $10 \cdot \log_{10}(\Sigma |O - R| / \Sigma |S - R|)$, where the summation occurs over all image pixels. For Figures 2a, 2b, and 2c $I = 3D$ 0.655277, for Figures 3a, 3b, and 3c $I = 6.714953$, and for Figures 4a, 4b, and 4c $I = 0.035239$.

The improvements are obvious and dramatic. Even Figure 4 shows some improvement, which is a bit surprising considering the amount of noise present. We expected the noise to significantly affect the center of mass calculation, which would degrade the algorithm's ability to reconstruct the missing high frequencies.

5. Conclusion

Our study suggests that random wander caused by atmospheric turbulence provides the necessary image displacement required by the super-resolution algorithm investigated. This is encouraging news to those using small telescope as a great difficulty with small telescopes is getting good resolution. The images obtained by researchers and amateurs can use super resolution with many astronomical objects. Another important aspect that many

small telescopes have, especially portable ones, is that the tracking is usually not that good. In addition many consumers buying telescopes usually get Alt-Az mounts. These mounts track along two axis and cause staircase movements to occur effecting long exposure CCD imaging. Since the images for super resolution do not have to be taken over several minutes, the Alt-Az tracking will affect the image quality.

We are currently working on the development of software to automate the image acquisition in order to further improve the results obtainable. In our next paper we will discuss these results.

REFERENCES

- Cheeseman, P., Kanefsky, B., Kraft, R., Stutz, J., & Hanson, R., 1996, Maximum Entropy and Bayesian Methods, G. R. Heidbreder, Kluwer Academic Publishers: Santa Barbara, 293
- Fruchter, A. S. & Hook, R. N., 2002, "Drizzle: A Method for the Linear Reconstruction of Undersampled Images" PASP, 114, 144
- Patti, A. J., Sezan, M. I., & Tekalp, A. M., 1995, Proceedings 1995 IEEE Int. Conf. Acoustics, Speech, & Signal Processing: Detroit, 2197
- Schultz, R. R. & Stevenson, R. L., 1994, IEEE Trans. Image Processing, 3, 3, 233
- Schultz, R. R. & Stevenson, R. L., 1996, IEEE Trans. Image Processing, 5, 6, 996
- Starck, J. L. & Pantin, E., 2002, PASP, 114, 1051
- Tatarskii, V. I. & Zavorotny, V. U., 1993, Journal of the Optical Society of America, 10, 11, 2410
- Troxel, S. E., Welsh, B. M., & Roggemann, M. C., 1995, Journal of the Optical Society of America, 12, 3, 570
- Tsai, R. Y. & Haung, T. S., 1984, Advances in Computer Vision and Image Processing, 1, R. Y. Tsai & T. S. Haung, JAI Press, Inc., 317

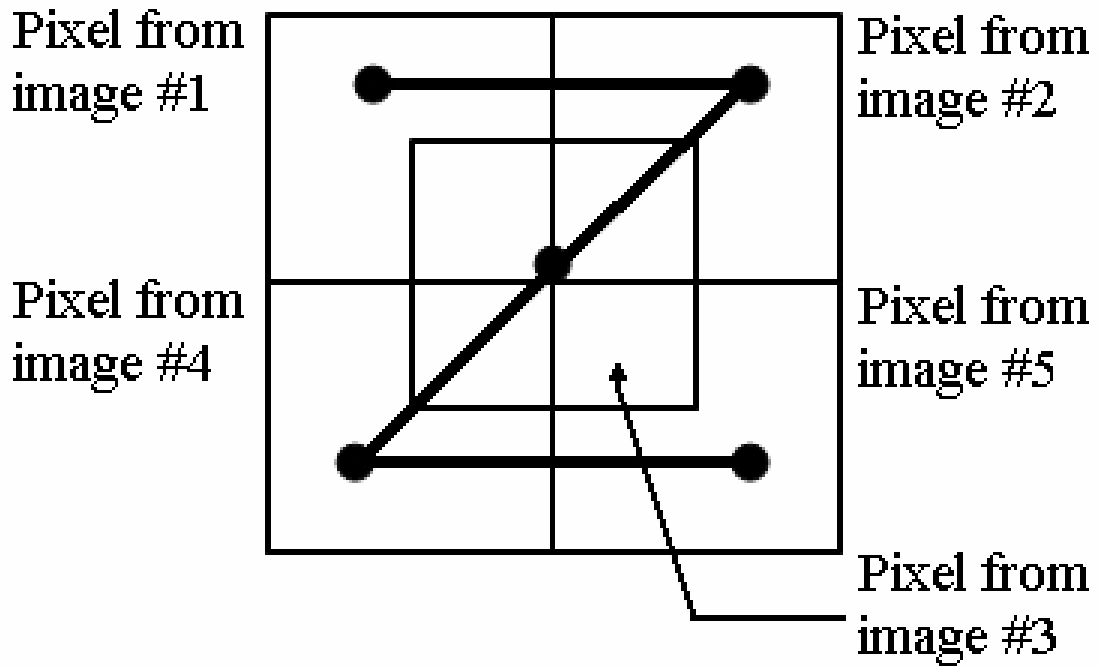


Fig. 1.— Ideal displacements.

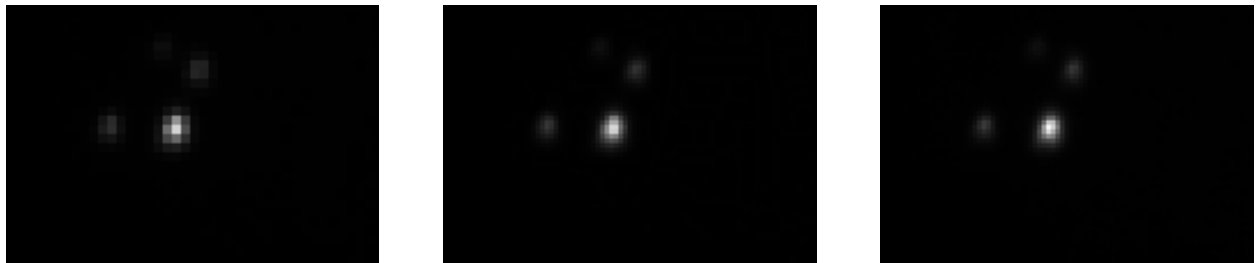


Fig. 2.— Orion constellation original image (a). Orion constellation super-resolution image (b). Orion constellation reference image (c).

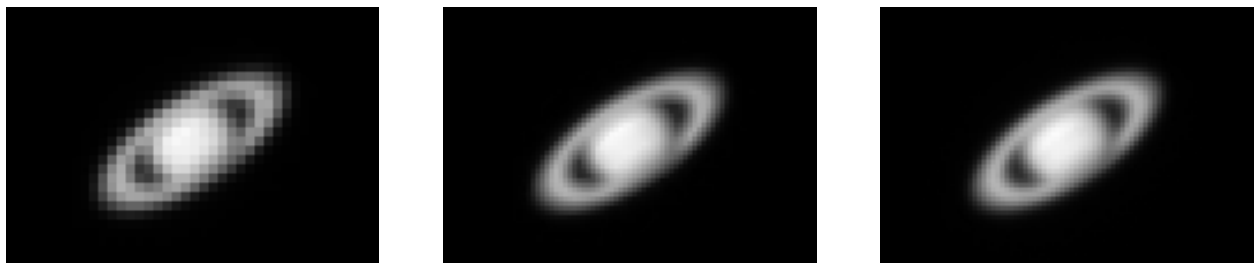


Fig. 3.— Saturn original image (a). Saturn super-resolution image (b). Saturn reference image (c).

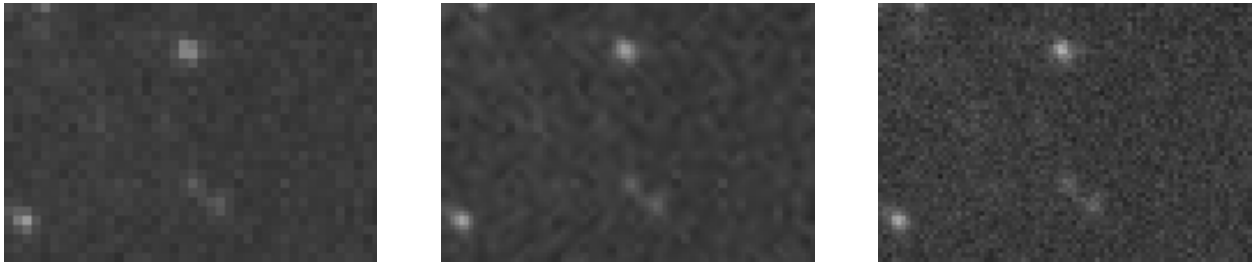


Fig. 4.— Hercules cluster original image (a). Hercules cluster super-resolution image (b). Hercules cluster reference image (c).